6. Concluding remarks

In the present paper we have shown that the problem of preferential distribution of Bi^{3+} ions in the [001]-oriented film of $Y_{3-x}Bi_xFe_5O_{12}$ garnet can be solved in a straightforward way using the XSW method. The same method may also be used for other orientations. We note, however, that in the case of the [111] growth direction the reflections with reciprocal-lattice vectors perpendicular to the surface cannot be used. This is related to the garnet crystallography: for [111]-oriented films different groups of the *c* sites lie in the same planes parallel to the surface and thus cannot be distinguished by the XSW method. In this case an inclined geometry is needed.

The XSW method may also be used to determine the preferential distribution of other kinds of ions, in particular the distribution of rare-earth and yttrium ions over dodecahedral sites may be determined. Finally, we note that if synchrotron radiation, rather than conventional X-ray tubes, were to be used the XSW method could provide a fast and efficient way for the determination of all kinds of preferential distributions of ions in garnet films.

References

BATTERMAN, B. W. (1964). *Phys. Rev. A*, **133**, 759–764.

BATTERMAN, B. W. (1969). *Phys. Rev. Lett.* **22**, 703–705.

BATTERMAN, B. W. & COLE, H. (1964). *Rev. Mod. Phys.* **36**, 681–717.

HANSEN, P. & KRUMME, J. P. (1984). *Thin Solid Films*, **144**, 69–107.

KAZIMIROV, A. YU., KOVALCHUK, M. V. & KOHN, V. G. (1988). *Sov. Tech. Phys. Lett.* **14**(8), 587–588.

KOVALCHUK, M. V. & KOHN, V. G. (1986). *Sov. Phys. Usp.* **29**, 426–446.

KOVALCHUK, M. V., KOHN, V. G. & LOBANOVICH, E. F. (1985). *Sov. Phys. Solid State*, **27**, 2034–2038.

KOZUMPLIKOVA, M., KUB, J. & SIMSOVA, J. (1983). *Proc. Third Course of Advanced Studies in EMA and REM*, pp. 174–178. Poljanka, Czechoslovakia.

KROLZIG, A., MATERLIK, G. & ZEGENHAGEN, J. (1983). *Nucl. Instrum. Methods*, **208**, 613–619.

LAGOMARSINO, S., SCARINCI, F. & TUCCIARONE, A. (1984). *Phys. Rev. B*, **29**, 4859–4863.

NEVRIVA, M., NOVAK, P. & CERMAK, J. (1985). *J. Cryst. Growth*, **71**, 409–418.

NOVAK, P. (1984). *Czech. J. Phys.* **B34**, 1060–1074.

PINSKER, Z. G. (1978). *Dynamical Scattering of X-rays in Crystals*. Berlin: Springer-Verlag.

WINKLER, G. (1981). *Magnetic Garnets*. Braunschweig: Vieweg.

ZHELUDEVA, S. I., ZAKHAROV, B. G., KOVALCHUK, M. V., KOHN, V. G., SOZONTOV, E. A. & SOSFENOV, A. N. (1988). *Sov. Phys. Crystallogr.* **33**(6), 804–807.

Acta Cryst. (1992). **B48**, 584–590

High-Temperature Neutron Powder Diffraction Study of $ZrSiO_4$ up to 1900 K

BY Z. MURSIC

Institut für Kristallographie der Universität, Theresienstrasse 41, 8000 *München* 2, *Germany, and Institut Laue–Langevin, BP* 156 *X*, 38042 *Grenoble CEDEX, France*

T. VOGT

Institut Laue–Langevin, BP 156 *X*, 38042 *Grenoble CEDEX, France*

AND F. FREY

Institut für Kristallographie der Universität, Theresienstrasse 41, 8000 *München* 2, *Germany*

(*Received* 3 *October* 1991; *accepted* 6 *March* 1992)

Abstract

We report here a high-temperature study of synthetic zircon up to 1900 K using high-resolution neutron powder diffraction in combination with a mirror furnace. Zircon ($ZrSiO_4$) is tetragonal, space group $I4_1/amd$, $Z = 4$, $a = 6.605$, $c = 5.987$ Å (room-temperature values). A previously unknown displacive structural change in the vicinity of 1100 K was detected. This 'transition' occurs in the temperature region where metamict zircon crystals recrystalize. Structural changes point towards the tilting of silicate tetrahedra as the driving force for this process. It is useful to describe the Zr—O polyhedral environment as two interpenetrating tetrahedra with a different temperature evolution rather than as a dodecadeltahedron. We have also followed the decomposition of $ZrSiO_4$ into tetragonal ZrO_2 and SiO_2 with the β-cristobalite structure. There is experimental evidence for the gradual disordering of the Zr—O subunit.

Introduction

Zirconium orthosilicate ($ZrSiO_4$) is dimorphous. Besides the dimorph characterized in the *Abstract*,

0108-7681/92/050584-07$06.00

there is a scheelite-type species. A review of the crystal structure is given, *e.g.* by Speer (1982). High-temperature structural studies of synthetic zircon are not available even though important technical applications rely on the high-temperature properties. $ZrSiO_4$ is an important refractory material due to its low coefficient of thermal expansion and high thermal shock resistance. To relate this to the structure and chemical bonding, structural studies at high temperatures are needed. So far the only known structural phase transition of $ZrSiO_4$ occurs under static pressure (Reid & Ringwood, 1969) or is shock induced (Kusaba, Takehiko, Kikuchi & Syono, 1986) from the zircon to the scheelite-type. A displacive mechanism for this was discussed by Kusaba *et al.* (1986). The mineral zircon occurs with different degrees of crystallinity due to radiation damage caused by radioactive decay of, mainly U and Th, atoms substituting Zr in the lattice. This so-called metamictization is crucial to radiometric age dating and the problems of radioactive waste storage (Headley, Ewing & Haaker, 1981). On heating metamict zircons anneal – a process that has attracted a lot of attention over the years (Weber, 1990, and references cited therein). The detailed structural changes during this recrystallization are unknown.

In a previous study (Mursic, Vogt, Boysen & Frey, 1992) we investigated this process in natural zircon using high-temperature single-crystal neutron diffraction. The present study was undertaken in order to search for structural changes in synthetic zircon in the temperature region where annealing of metamict zircon takes place. The highly disordered state of $ZrSiO_4$ may be characterized by local structures which are considerably different from vitreous Zr-bearing silicates (Brown & Ponader, 1986). Therefore, one should look closer at the phenomena of metamictization and annealing of metamict minerals in relationship to the structural behaviour of their synthetic crystalline counterparts. As pointed out by Hawthorne *et al.* (1991) annealing will restore the initial crystalline structure at low degrees of radiation damage since the local structure present in small domains of aperiodic material embedded in the crystalline matrix requires only small atomic displacements to recrystallize and the surrounding matrix constrains the movements.

Experimental

The neutron powder diffraction experiments were carried out on the high-resolution powder diffractometer D2B at the ILL in Grenoble (Hewat, 1986). We used a wavelengh of 1.594 Å. The mirror furnace was the same as that used in previous ZrO_2 studies (Frey, Boysen & Vogt, 1990; Boysen, Frey & Vogt, 1991). The sample, which was purchased from K&K Labs (a division of ICN Biomedicals Inc., Ohio), was held in a Pt container and placed at the common focus of two ellipsoidal mirrors equipped with two 1000 W halogen lamps. As thermocouples we used Pt/Pt–10% Rh. Temperature control was achieved *via* a PID controller with a thyristor regulating the lamp current. The temperature was stable within ±3 K. On an absolute scale we estimated the error to be 3%.

The data were analysed using the Rietveld refinement program *PROFIL* written by Cockcroft (1987). The background was determined by a linear interpolation between regions without Bragg reflections. The measured intensities used in the program are the measured counts minus the background.

Results

Fig. 1. shows the refined diffraction pattern at room temperature (*a*) and at 1900 K (*b*) after the decomposition had started. This is indicated by the ZrO_2 peaks (lower tick marks). The platinum peaks (black dots) could easily be distinguished and were excluded from the refinement. Plotting the scale factor against temperature shows a noticeable decline above 1100 K (Fig. 2). This is consistent with the creation of disorder and/or an increase in thermal diffuse scattering. The rapid decrease of the scale factor at temperatures above 1750 K is due to the increased diffuse scattering of β-cristobalite, which is one of the products of the decomposition. The variation of cell constants and cell volume with temperature clearly show an anomaly near 1100 K. Above and below we were able to fit the data sets with a polynominal of degree two: $x = A_0 + A_1T + A_2T^2$ (Fig. 3). Between room temperature and 1100 K the temperature dependency of the *a* axis could be fitted by the coefficients $A_0 = 6.6003\ (3)$, $A_1 = 126\ (8) \times 10^{-7}$, $A_2 = 82\ (5) \times 10^{-10}$. Between 1500 and 1800 K $A_0 = 6.65\ (2)$, $A_1 = -4\ (2) \times 10^{-5}$ and $A_2 = 24\ (8) \times 10^{-9}$. For the *c* axis the coefficients between room temperature and 1100 K are $A_0 = 5.9783\ (3)$, $A_1 = 29\ (1) \times 10^{-6}$ and $A_2 = 67\ (8) \times 10^{-10}$; between 1400 and 1800 K $A_0 = 6.05\ (1)$, $A_1 = -5\ (1) \times 10^{-5}$, $A_2 = 28\ (4) \times 10^{-9}$. The cell constants were then used to derive the thermal expansion coefficients α_a and α_c.*

Fig. 4 displays their thermal evolution and the significant change near 1100 K. The almost linear increase of both expansion coefficients changes into a slower nonlinear increase in α_a and a decrease in α_c between 1100 and 1600 K.

* Lists of powder diffraction data and refined parameters have been deposited with the British Library Document Supply Centre as Supplementary Publication No. SUP 55086 (43 pp.). Copies may be obtained through The Technical Editor, International Union of Crystallography, 5 Abbey Square, Chester CH1 2HU, England.

The most important features helping to clarify the structural changes are the bond distances and angles as well as the polyhedral volumes. Fig. 5 shows the evolution of the Si—O bond length and the resulting expansion of the tetrahedral volume with temperature. One can see that while the Si—O bond and tetrahedral volume expand near 1100 K, the volume increase of the ZrO_8 dodecadeltahedron is hardly changed (Fig. 6). The Zr—O(I) distance remains constant within the temperature region where the transition takes place and increases afterwards, whereas the Zr—O(II) distance increases steadily and one observes only a very small change in the slope of the bond length *versus* temperature plot as seen in Fig. 7(*a*). Other parameters such as atomic displacement parameters and the parameters describing the instrumental resolution convoluted with the sample-dependent effects (mainly strain and particle-size broadening) also show anomalies near 1100 K. Fig. 8 displays the temperature-dependent values of the equivalent isotropic atomic displacement parameters. Extrapolating the data below 1100 K down to 0 K all of them show behaviour expected by the Debye approximation. All three values show a distinct anomaly at 1100 K.

The decomposition of $ZrSiO_4$ is indicated by the observation of new peaks at 1750 K. A two-phase refinement using the tetragonal modification of ZrO_2 as second phase converged. No traces of a third

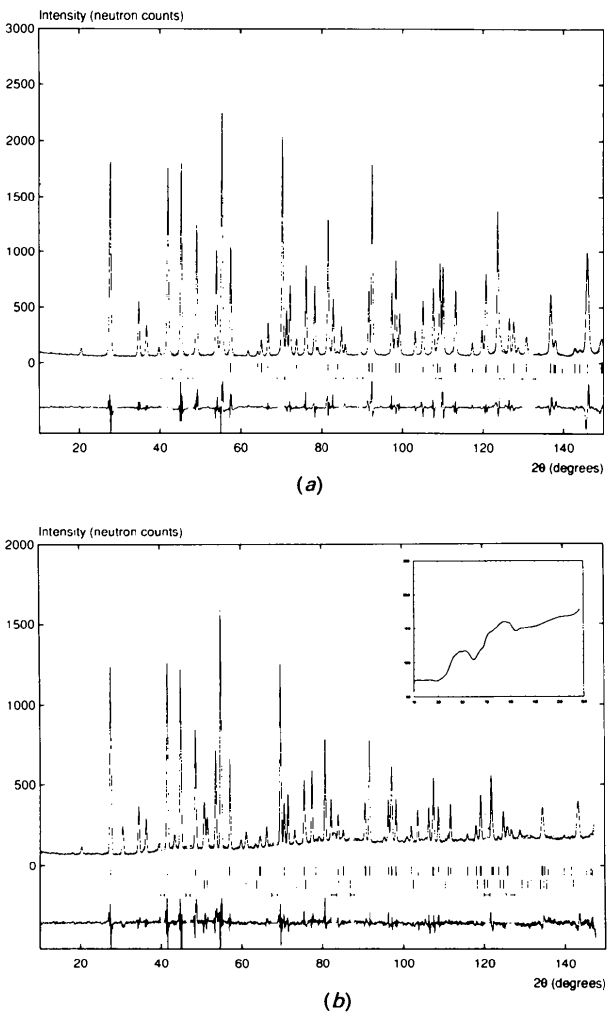

Fig. 1. Refined diffraction pattern of $ZrSiO_4$ at (*a*) room temperature and (*b*) 1900 K. The tick marks indicate the Bragg peaks (at 1900 K the upper ones are for $ZrSiO_4$, the lower ones for tetragonal ZrO_2). The excluded regions are those with Bragg peaks steming from the Pt sample holder. The inset shows the diffuse background scattering on a different scale. It is very similar to that of β-cristobalite (Vogt & Schmahl, 1992).

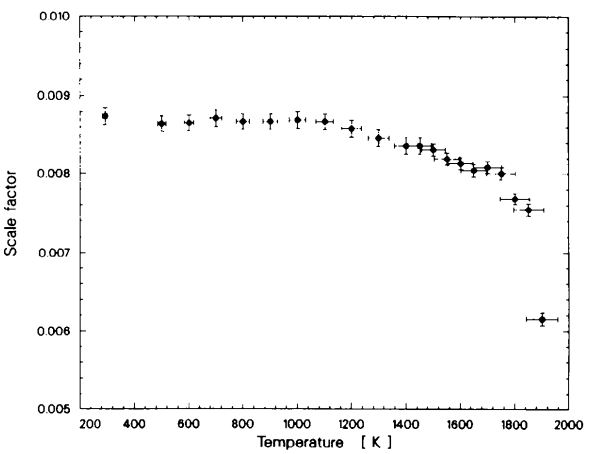

Fig. 2. Scale factor *versus* temperature indicating the structural transition at 1100 K and the decomposition at 1750 K.

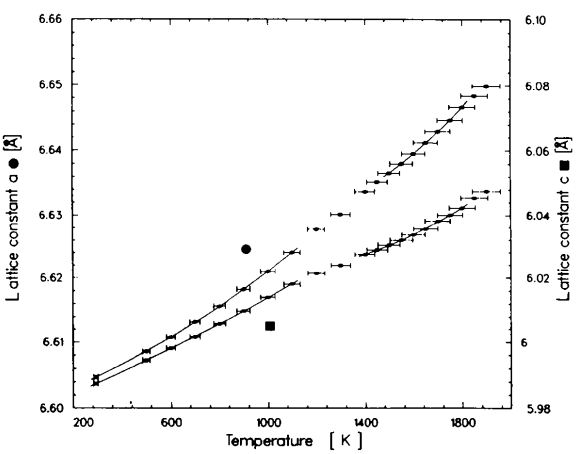

Fig. 3. Cell constants *versus* temperature showing anomaly at 1100 K.

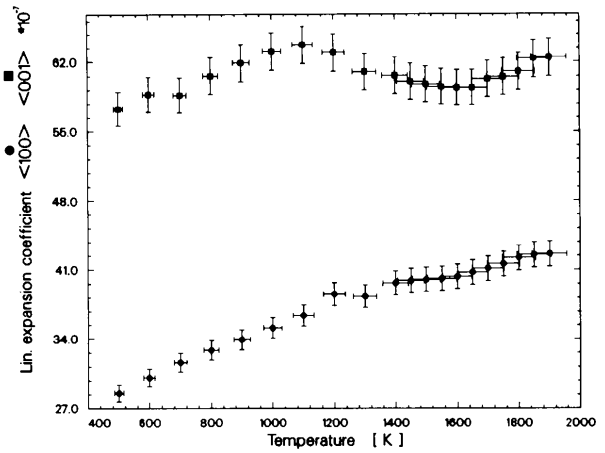

Fig. 4. Thermal expansion coefficients.

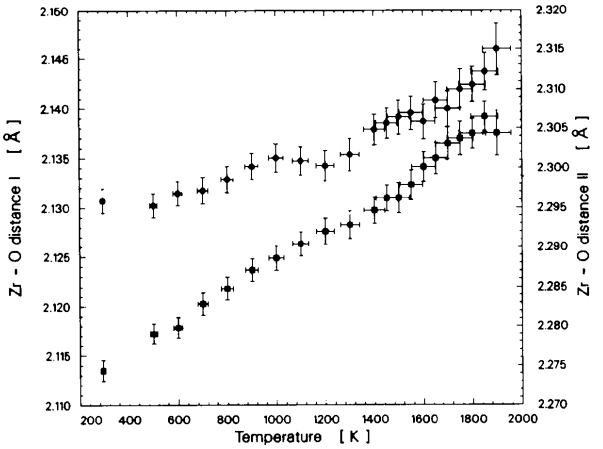

(*a*)

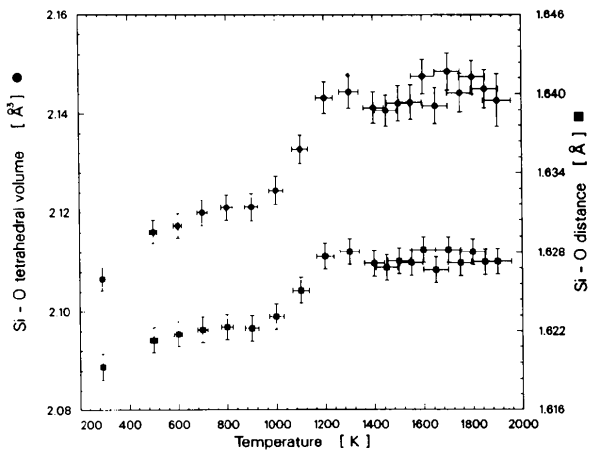

Fig. 5. Evolution of the Si–O bond distance and SiO_4 tetrahedral volume with temperature.

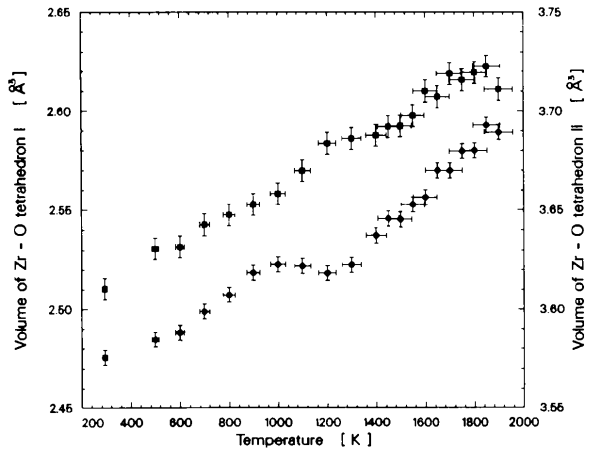

(*b*)

Fig. 7. The different thermal response of the two ZrO_4 tetrahedron volumes and Zr—O distances.

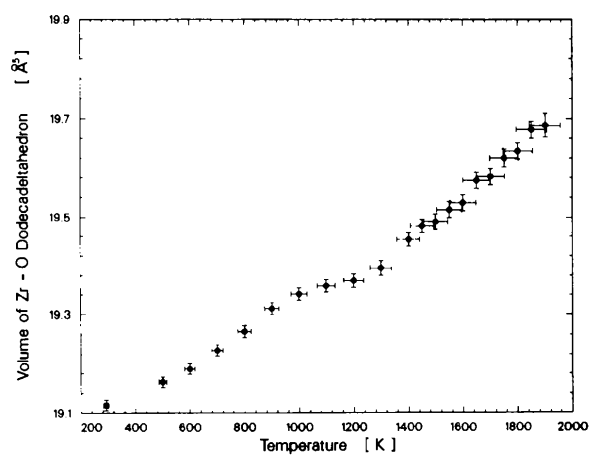

Fig. 6. Thermal evolution of the ZrO_8 dodecadeltahedron.

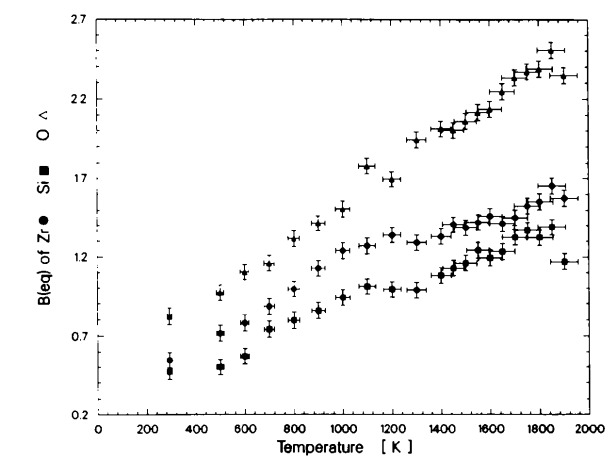

Fig. 8. Thermal evolution of the atomic displacement parameters in $ZrSiO_4$.

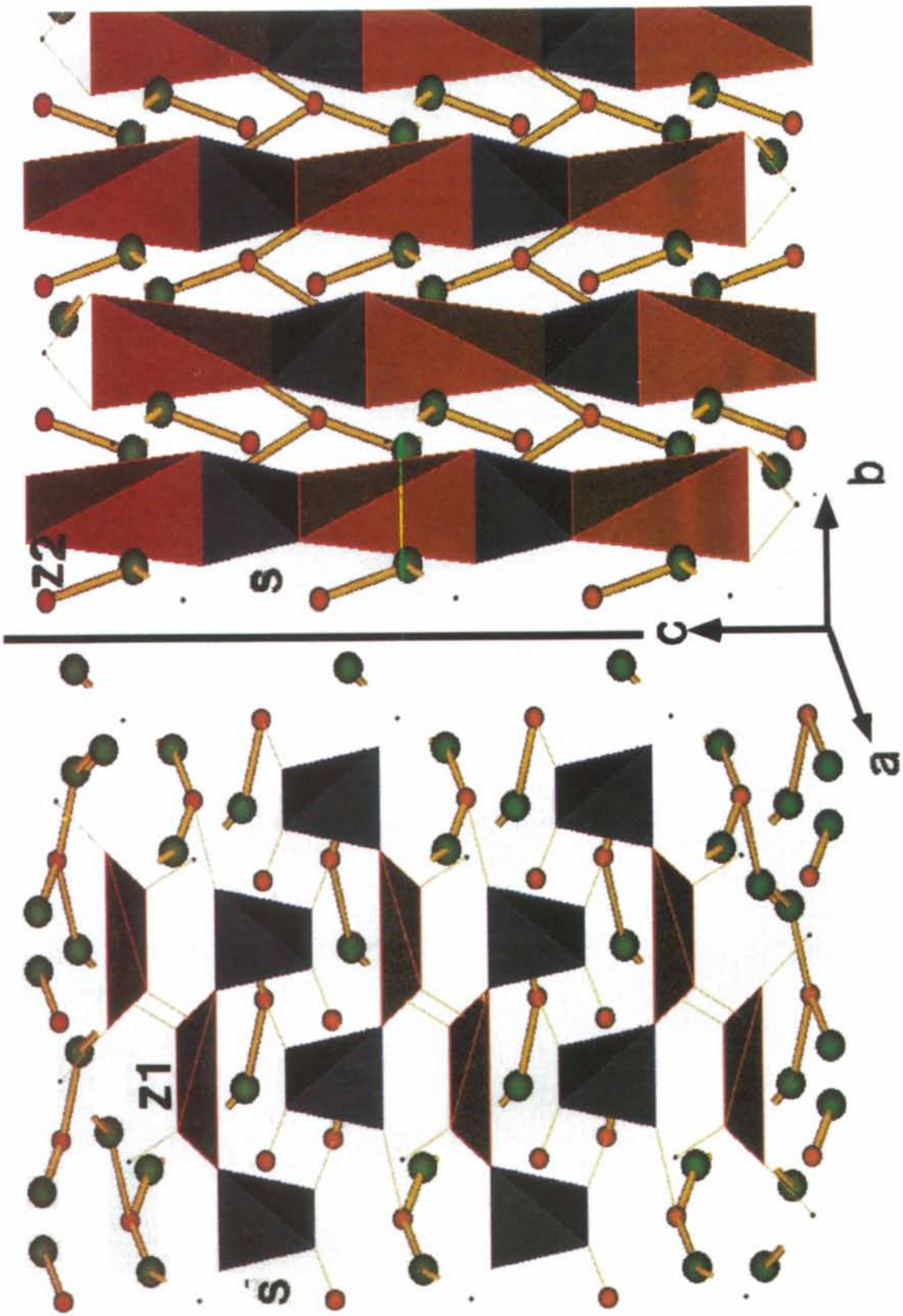

Fig. 9. Structural description of $ZrSiO_4$ using two ZrO_4 tetrahedra, one corner-linked (Z1), the other edge-connected (Z2) to the silicate tetrahedra (S).

phase were observed. The evolution of the β-cristobalite phase is probably time-dependent. The diffuse background of this phase (see inset in Fig. 1) is visible in the early stages of the decomposition indicating an amorphous state of small and possibly disordered particles of the β-cristobalite phase. Having measured β-cristobalite on the same instrument we recognized the very pronounced diffuse scattering which modulates the background. Analysis of the scale factors of the two phases shows that at 1900 K roughly 15% of tetragonal ZrO_2 coexists with $ZrSiO_4$. This number should not be taken without caution since we have no way of determining the amount of amorphous SiO_2 and the time dependency of the decomposition.

Discussion

Zircon is made up of isolated SiO_4 tetrahedra which are separated by Zr atoms bonded to eight oxygens forming a dodecadeltahedral coordination polyhedron. These two polyhedra are edge-sharing and alternate along the *c* axis. Adjacent rows of polyhedra along the *a* and *b* axis are also connected *via* edge-sharing of the ZrO_8 dodecadeltahedra. Another way of looking at the structure is to take advantage of the geometrical fact that a dodecadeltahedron can be constructed from two interpenetrating tetrahedra (Nyman, Hyde & Andersson, 1984). Hence one accounts for the fact that in the ZrO_8 dedecadeltahedra two different Zr—O distances create a ZrO_{4+4} rather than a uniform ZrO_8 coordination. One of the ZrO_4 tetrahedra is squashed and has a smaller Zr—O distance, the other is elongated with a larger Zr—O distance. We refer to these distances as Zr—O(I) and Zr—O(II), respectively. Analyzing the zircon structure using the two different ZrO_4 tetrahedra together with the SiO_4 tetrahedra as building units, one sees that the smaller squashed tetrahedra are corner-linked along the *c* axis to the SiO_4 tetrahedra whereas the elongated larger ones are edge-linked in the *ab* plane (Fig. 9). It is obvious that the thermal behaviour of corner- and edge-linked units is very different (Fig. 7). The edge-sharing tetrahedra are coupled very rigidly constraining the temperature behaviour of the individual tetrahedra, whereas the corner-sharing topology of tetrahedra can to a certain degree allow different temperature behaviour. Using this to describe the structure, the structural disortions at high temperatures can be more easily understood. The increase in the dodecadeltahedral volume is mainly due to the steady increase of the Zr—O(II) distance. This represents the larger edge-sharing tetrahedron. Even in the temperature range 1000–1200 K only a slight change in the slope of the bond distance *versus* temperature plot is seen (Fig. 7*a*). On the other hand the Zr—O(I) bond corresponding to the smaller squashed tetrahedra does not expand at all during the transition period (Fig. 7*b*). In the same temperature range the Si—O bond and with it the tetrahedral volume show a dramatic increase towards a value at which they remain until decomposition (Fig. 5). The corner-sharing tetrahedra [ZrO(I)] are able to respond to the force created by this expansion of the SiO_4 tetrahedron *via* a rotation which leaves the bond distance almost unchanged. The edge-sharing ZrO_4 tetrahedra [ZrO(II)] do not have this degree of freedom and thus the bond distance increases continuously following the expansion of the SiO_4 tetrahedron. The rotation of the smaller tetrahedron is also reflected in the decrease of the linear expansion coefficient α_c (Fig. 4). Both Zr—O distances continue to increase after the transition. At around 1500 K the tetrahedral angles of the SiO_4 group start to approach the angles of an ideal tetrahedron (Fig. 10). We understand this in terms of a gradual breakdown of the Zr—O dodecadeltahedral subunit due to increasing incompatability of the two Zr—O bonds of the two interpenetrating tetrahedra. The stability limit of this subunit is reached and it minimizes the free energy by rearranging to give an eightfold coordination of Zr in tetragonal ZrO_2. This new structural arrangement accommodates greater differences between the two Zr—O bonds. The SiO_4 tetrahedra on the other hand are known to exist even in the melt at temperatures beyond 3000 K. The more unstable the Zr—O subunit becomes the less geometrical constraints affect the silicate tetrahedra and the more they approach an ideal tetrahedral geometry. The decomposition can thus be described as the structural rearrangment of the Zr—O subunit which is no longer compatible with the Si—O subunit. The Si—O subunit then rearranges into an SiO_2 structure which has its stability field at high temperatures, *i.e.*

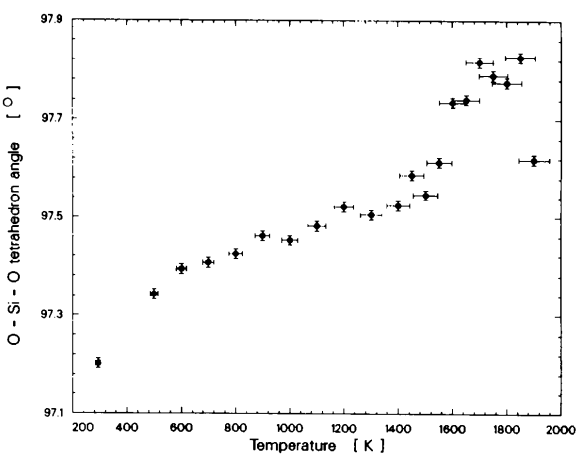

Fig. 10. Thermal evolution of the silicate tetrahedral angle.

the β-cristobalite structure. The well-known diffuse background of this compound (Vogt & Schmahl, 1992) is observed well before any Bragg scattering (Fig. 1). This leads to the suggestion that the decomposition proceeds either *via* an amorphous SiO_2 phase or, possibly, the β-cristobalite structure is realized only over a few cells leading to very broad reflections caused by the small coherence length. The subtle shifts and changes occurring in the coordination of the cations between 1000 and 1200 K classify this structural transition as a displacive one involving polyhedral tilt despite the fact we do not observe any symmetry change (Hazen & Finger, 1982). After the diffraction experiments we performed differential scanning calorimetry measurements on a sample from the same batch. The differential scanning calorimetry curve shows evidence of three very sluggish exothermal heat peaks. A small peak near 650 K, a second small peak near 1100 K, the temperatures at which our data suggest the start of the phase transition, and a third major peak near 1400 K corresponding to the end of the transition and the beginning of an increase in the O—Si—O tetrahedral angle indicating some precursor effect of the following decomposition.

This new view of the structural rearrangement in $ZrSiO_4$ around 1100 K sheds new light on the phenomena of metamictization and the annealing of metamict zircon. A model of metamictization proposed by Farges & Calas (1991) assumed tilting of the SiO_4 tetrahedra to explain the lower coordination number of Zr in the metamict state as observed by their EXAFS studies. This also agrees with the results of infrared spectroscopy measurements of metamict zircons performed by Woodhead, Rossman & Silver (1991). They observed a broadening of the fundamental and combination modes depending on the internal SiO_4 vibrations indicating tilting and/or rotation of the silicate tetrahedra. IR bands which to a first approximation are mainly dependent on the Si—O bonds remain unchanged during metamictization whereas those dependent mainly on the Zr—O bonds disappeared. Thus metamictization can be seen as a disorder phenomenon where the Zr—O subunit dissolves and the silicate tetrahedra adapt to this disorder by tilting. This explains the less efficient packing, the increase in cell volume and the decrease in density – all properties associated with metamictization (Holland & Gottfried, 1955). The annealing of metamict zircon can thus be viewed as a reordering process where the ability of the silicate tetrahedra to rotate and tilt induces the reestablishment of the Zr—O subunit. It seems plausible that anomalies in the dynamic behaviour trigger this reordering process. Experiments to verify this are underway.

Concluding remarks

It has been shown that the high-temperature structural changes of $ZrSiO_4$ can be understood by describing the ZrO_8 entity as two interpenetrating tetrahedra instead of one dodecadeltahedron. A reordering process induced by the tilting of silicate tetrahedra has been observed in a temperature range which coincides with the annealing temperature of metamict zircon. This allows an important effect to be placed on a more sound structural basis. The main feature is that the increase in volume of the SiO_4 tetrahedra induces a rotation of the corner-linked ZrO_4 tetrahedra. Both processes, the metamictization and decomposition of zircon are intimately related to the structural instability of the Zr—O subunit and in both cases the coordination polyhedra are rearranged. In the case of metamictization the coordination number seven is preferred and a local structure close to the one adopted in baddeleyite (monoclinic ZrO_2) is taken on (Farges & Calas, 1991), whereas in the decomposition a stable ZrO_8 arrangement is achieved by rearranging to the stable tetragonal ZrO_2 structure. In both cases the silicate tetrahedron is preserved as a structural entity.

References

BOYSEN, H., FREY, F. & VOGT, T. (1991). *Acta Cryst.* **B47**, 881–886.

BROWN, G. E. JR & PONADER, C. W. (1986). *Int. Mineral. Assoc. Abstr.* p. 63.

COCKCROFT, J. K. (1987). *PROFIL.* Unpublished Rietveld program.

FARGES, F. & CALAS, G. (1991). *Am. Mineral.* **76**, 60–73.

FREY, F., BOYSEN, H. & VOGT, T. (1990). *Acta Cryst.* **B46**, 724–730.

HAWTHORNE, F. C., GROAT, L. A., RAUDSEPP, M., BALL, N. A., KIMATA, M., SPIKE, F. D., GABA, R., HALDEN, N. M., LUMPKIN, G. R., EWING, R. C., GREGOR, R. B., LYTLE, F. W., ERCIT, T. S., ROSSMAN, G. R., WICKS, F. J., RAMIK, R. A., SHERIFF, B. L., FLEET, M. E. & MCCAMMON, C. (1991). *Am. Mineral.* **76**, 370–396.

HAZEN, R. M. & FINGER, L. W. (1982). *Phase Transit.* **1**, 1–22.

HEADLEY, T. J., EWING, R. C. & HAAKER, R. F. (1981). *Nature (London)*, **293**, 449–450.

HEWAT, A. W. (1986). *Mater. Sci. Forum*, **9**, 69–80.

HOLLAND, H. D. & GOTTFRIED, D. (1955). *Acta Cryst.* **8**, 291–300.

KUSABA, K., TAKEHIKO, Y., KIKUCHI, M. & SYONO, Y. (1986) *J. Phys. Chem. Solids*, **47**, 675–679.

MURSIC, Z., VOGT, T., BOYSEN, H. & FREY, F. (1992). *J. Appl. Cryst.* **25**, 519–523.

NYMAN, H., HYDE, B. G. & ANDERSSON, S. (1984). *Acta Cryst.* **B40**, 441–447.

REID, A. F. & RINGWOOD, A. E. (1969). *Earth Planet. Sci. Lett.* **44**, 390.

SPEER, J. A. (1982). In *Reviews in Mineralogy*, Vol. 5, *Orthosilicates*, edited by P. H. RIBBE. Washington, DC: Mineralogical Society of America.

VOGT, T. & SCHMAHL, W. W. (1992). To be published.

WEBER, W. J. (1990). *J. Mater. Res.* **5**, 2687–2697.

WOODHEAD, J. A., ROSSMAN, G. R. & SILVER, L. T. (1991). *Am. Mineral.* **76**, 74–82.